Effect of Magnesium Oxide on Physical and Biological Properties in β-tricalcium Phosphate Ceramic

Effect of Magnesium Oxide on Physical and Biological Properties in β-tricalcium Phosphate Ceramic

M. Chuthathip[1,3], M. N. Ahmad-Fauzi [1], B. I. Yanny-Marliana[1], S. Khairul-Anuar[1], K. Masakazu[2], L. Banhan[3]

[1]Biomaterials Niche Group, School of Materials and Mineral Resources Engineering, Universiti Sains Malaysia, Penang 14300, Malaysia

[2]Graduate School of Biomedical Engineering, Tohoku University, Sendai 980-8579, Japan

[3]Department of Industrial Engineering, Faculty of Engineering, Burapha University, Chonburi 20131, Thailand

Email: srafauzi@usm.my

Abstract. β-TCP is bioresorbable ceramic which has excellent osteoinduction and osteoconduction properties for using as bone cement and bone implant material. However, their natural brittleness and insufficient compaction after sintering under the transformation phase from β- to α-TCP limit their utility for clinical performance. The purpose of this work is to investigate the effect of magnesium ion as the doping element on the β-TCP. The experiment was conducted by introduced 1.0wt% of MgO into the β-TCP structure via simultaneous balls milling and mixing method. Afterward, the powders were pressed into pellets and went through conventional sintering method. The sintered samples were examined by powder X-ray diffraction (XRD), density and biological test for investigation.

1. Introduction

Tricalcium phosphate (TCP) has three polymorphs: β-TCP is stable below 1180°C, α-TCP from 1180°C to 1400°C, and ά-TCP above 1470°C. β-TCP is the preferred phase as a bioceramic substituting graft material due to its good chemical stability and proper bioresorption rate [1]. The low mechanical strength of β-TCP ceramic is, however, an essential concern to use these ceramics as surgical implants. Hence, it is important to improve the mechanical properties by densifying β-TCP ceramics fully since the sintering temperature should be lower than the phase transition of β-to α-TCP [2]. Magnesium is an essential element in the human body, with about 65% of total body magnesium is contained in bone and teeth. An adverse depletion of magnesium affects all stage of skeletal metabolism consequently decreasing bone growth, osteoblastic and osteoclastic activities [3]. Doping of calcium phosphate materials with Mg could improve osteoblastic cellular attachment, proliferation and ALP production. It has been reported that Mg can be incorporated into TCP structure by substitution of Ca and improves the thermal stability of TCP which prevents phase transformation at

high temperature [4]. Mg has been used clinically in magnesium phosphate bone cement and in several different bioglass compositions. In this work, the influences of MgO on physical and biological properties of bulk commercial TCP were investigated.

2. Experimental

2.1 Sample preparation

The samples were prepared by mixing 50 g β-TCP commercial powder (Sigma-Aldrich) with an appropriate amount of 1.0 wt% MgO (Sigma-Aldrich) [5] in a 500 ml polypropylene bottle containing 200 ml deionized water and 500 g of 13 mm diameter cylindrical zirconia milling media. The mixtures were milled for 24 hr at 150 rpm and dried in an oven at 100 °C for 24 hr, followed by grinding and sieving to obtain fine powders. Then, 0.8 g of the powders were pressed into a pellet in 14 mm diameter stainless steel mold using a uniaxial press (Specac) by 150 MPa. Finally, the green pellets were sintered at different temperatures (1100°C, 1150°C, 1200°C, 1250°C and 1300°C) by 20°C/min of heating rate and 2 hr of soaking time then cooled down by air atmosphere in the muffle furnace (Lenton UAF 15/15).

2.2 Phase analysis

Phase analysis of sintered doped and undoped β-TCP samples was carried out by powder X-ray diffraction (XRD) (Bruker D2 Phaser) with a copper anode (CuKα, λ=1.5406 Å) target. Each run was performed with 2θ values of 10-90° with a scan rate of 0.5 °/min.

2.3 Linear shrinkage, apparent porosity and relative density measurements

The diameter and thickness of pellets were measured before and after sintering to calculate the linear shrinkage. While the relative density and total porosity were evaluated using Archimedes method. The experiment procedure of density and porosity measurement was carried out according to the ASTM-C830 [6].

2.4 Biological test and microstructure analysis

The bioactivity of β-TCP has is normally evaluated by the ability of apatite formation in simulated body fluid (SBF) which relies on their ability to induce hydroxyapatite (HA) formation [7]. In this work, the SBF solution was prepared according to ISO 23317:2012 (E) [8] and the immerse duration was 3 weeks. Field emission scanning electron microscope (FESEM, ZEISS SUPRA 35VP) was employed to observe the surface morphologies of bone-like apatite layer of sintered TCP and MgO-TCP samples.

3. Results and discussion

3.1 Phase analysis

The XRD patterns of TCP and MgO-TCP samples are shown in Fig. 1 and 2. The spectrums of all samples (Fig. 1) matched well with the Inorganic Crystal Structure Database (ICSD) no. 97500 of β-TCP. Likewise, the spectrums of MgO-TCP (Fig. 2) also exhibited the single phase of β-TCP without the presence of α-TCP phase. It had been documented the β-TCP phase undergoes allotropic conversion to α-TCP beyond 1180°C and the presence of Mg^{2+} in its crystal lattice delay the allotropic conversion till 1400°C [9]. In this study, from the XRD analysis of sintered TCP and Mg-TCP sample presented the single pages of β-TCP even at high sintering temperature at 1300 °C. This suggests that

due to the starting material was commercial β-TCP so the sintered samples have a stable phase although sintered at high temperatures. In addition, a shifting in the 2θ and the d-spacing value for doped TCP corroborates the substitution of Ca^{2+} with Mg^{2+} in the β-TCP lattice [5]. The ionic radius of Mg^{2+} (0.69 Å) is smaller than that of Ca^{2+} (0.99 Å), leads to a decrease in the unit cell parameters of the β-TCP lattice, and therefore the shift in the peak to higher 2θ value occurred [10]. Hence, the shifting of the highest intensity diffraction peak at (0 2 10) to higher 2θ of MgO-TCP compared with TCP was observed as shown in Fig. 3. In addition, the shifting of peak to lower 2θ was noticed for both TCP and MgO-TCP samples. Particularly in MgO-TCP samples (Fig. 4), the diffraction peak at (0 2 10) shifted to lower 2θ as sintering temperature increased. This can be accounted as in the higher sintering temperature, an atomic mobility would increase and caused grain growth, which results in the better crystallinity and densification of samples [11, 12].

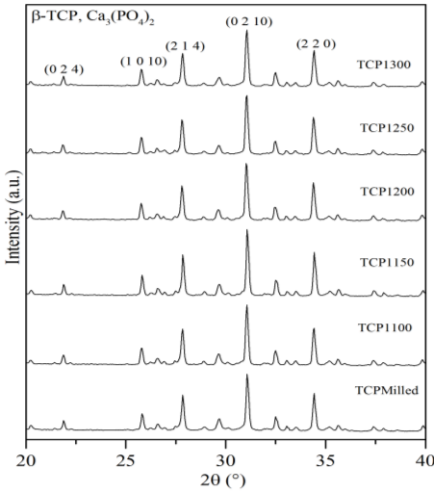

Figure 1. XRD pattern of milled powder and sintered TCP at different temperatures.

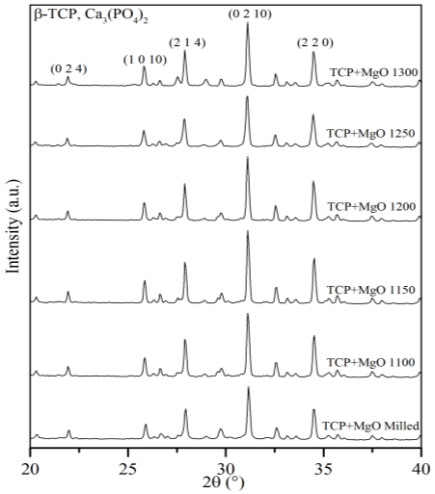

Figure 2. XRD pattern of milled powder and sintered MgO-TCP at different temperatures.

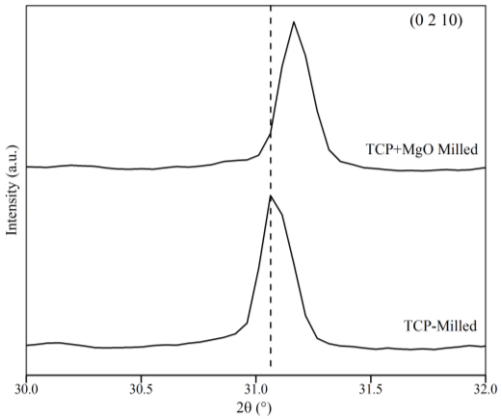

Figure 3. Peak shifted observation of milled TCP and MgO-TCP by XRD in the length of 2θ =30° to 32°.

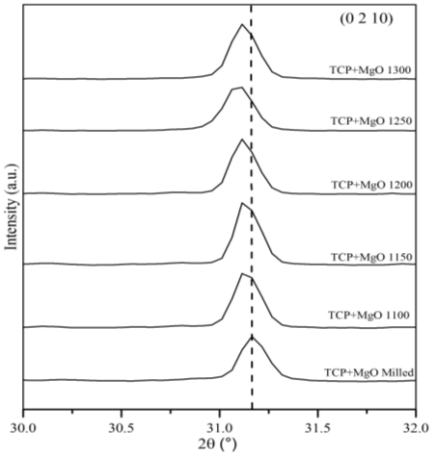

Figure 4. Peak shifted observation of sintered MgO-TCP by XRD in the length of 2θ =30° to 32°.

3.2 Linear shrinkage measurement

The linear shrinkage in diameter and thickness of sintered samples are shown in the Fig. 5 and 6, respectively. Generally, the shrinkage in both dimensions was rapidly increased as sintering temperature increased. However, at the temperature from 1250°C to 1300°C of TCP samples, the

diameter shrinkage slightly decreased (Fig. 5), while there is a small increase in thickness shrinkage at the same temperatures (Fig. 6). Conversely, the MgO-TCP samples showed slightly increased in diameter shrinkage (Fig. 5) while slightly decreased in thickness shrinkage (Fig. 6) at the temperature from 1250°C to 1300°C.

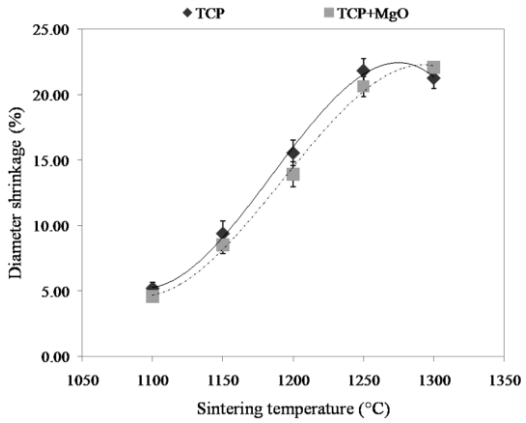

Figure 5. Diameter shrinkage of sintered TCP and MgO-TCP at different temperatures.

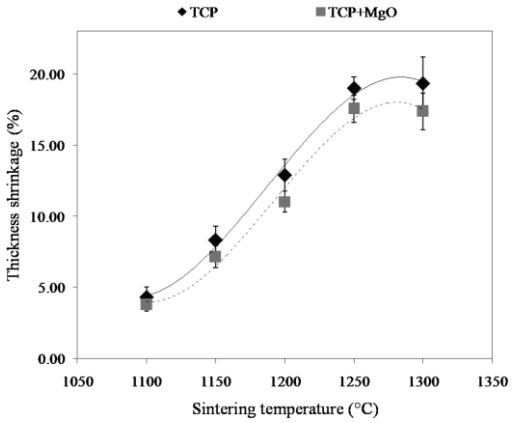

Figure 6. Thickness shrinkage of sintered TCP and MgO-TCP at different temperatures.

3.3 Apparent porosity and relative density measurement

Generally, the total porosity of both sintered TCP and MgO-TCP samples decreased in higher sintering temperature (Fig. 7) which well corresponded with the increase of relative density in the Fig.8. However, the sintered TCP samples showed better porosity and density than the sintered MgO-TCP samples except at the sintering temperature at 1300°C. Interestingly, although the XRD analysis of sintered TCP samples could not detect the α-TCP phase at a high sintering temperature of 1300 °C it clearly presented lower properties of linear shrinkage and density and porosity test compared with sintered MgO-TCP samples. These can be suggested that the α-TCP phase has started to form in the sintered TCP sample at 1300°C but could not detect by XRD analysis due to a very small quantity of α-TCP phase. Moreover, the expansion of sintered TCP during high sintering temperature causes micro-crack which consequently reduces the density property [13]. Since the Mg has the ability to stabilize β-TCP under high sintering temperature by delay the β-to α-phase transformation, the sintered MgO-TCP samples presented the better density and porosity result at the temperature of 1300°C.

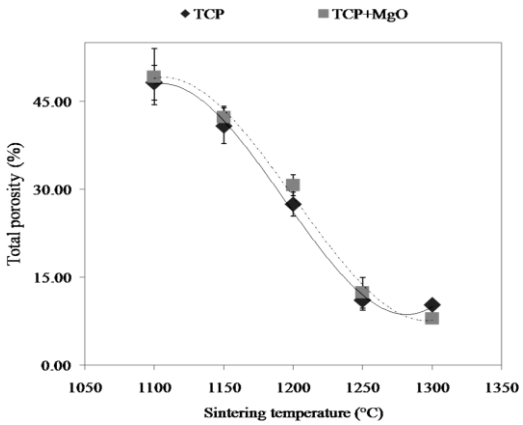

Figure 7. The total porosity of sintered TCP and MgO-TCP samples at different temperatures.

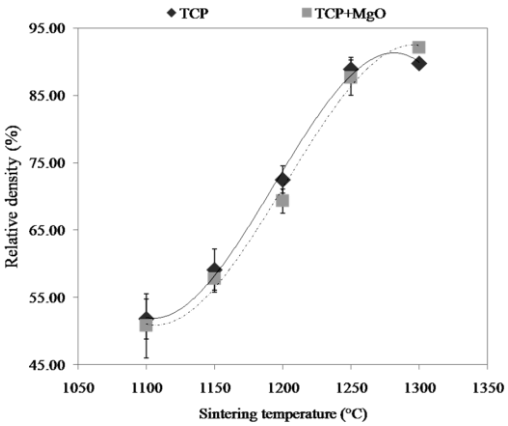

Figure 8. The relative density of sintered TCP and MgO-TCP samples at different temperatures.

3.4 Biological test and microstructure analysis

The investigation of the apatite formation ability of bioceramics in simulated body fluid (SBF) is an original protocol developed by Kokubo et al. [7]. The apatite formations were not observed on the sample surface of sintering temperature at 1100°C, 1150°C and 1200°C (Fig. 9 and 10: a, b, c) but can be seen on the sample surface of 1250 °C and 1300°C in both TCP (Fig. 9d and e) and MgO-TCP samples (Fig. 10d and e). The absent and negligible apatite formation of MgO-TCP samples due to the addition of magnesium into the β-TCP structure. It has reported that magnesium inhibited in vitro apatite formation which effects on the nucleation and crystal growth of calcium phosphates. Since the magnesium substituted into calcium site of β-TCP structure hence they inhibit nucleation of Ca-P phases and disrupt adsorption at active growth site. This kinetically consequently hinder nucleation of hydroxyapatite which results to formation of the apatite layer on the sintered MgO-TCP samples [14-18]. In addition, on the surface of sintered TCP at 1250°C exhibited predominant dense apatite formation which suggests it was the later stage for each granule grows bigger and becomes predominantly plate-like crystals (Fig. 9d) [13]. The apatite formation with similar morphologies has been reported in previous studies [19, 20].

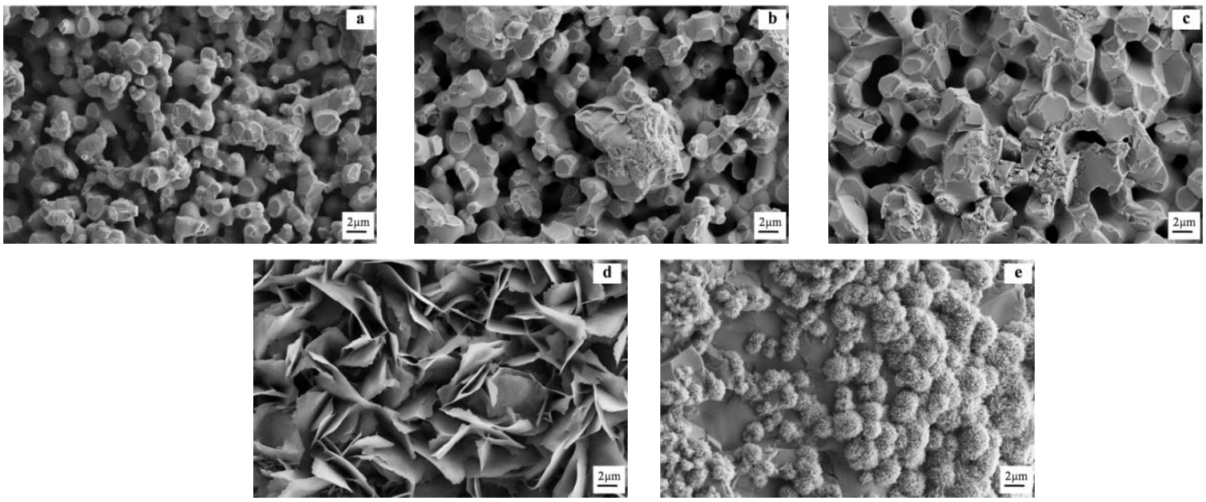

Figure 9. Surface morphology of sintered TCP after immersed in SBF for 3 weeks: (a) 1100°C; (b) 1150°C; (c) 1200°C, (d) 1250°C; and (e) 1300°C.

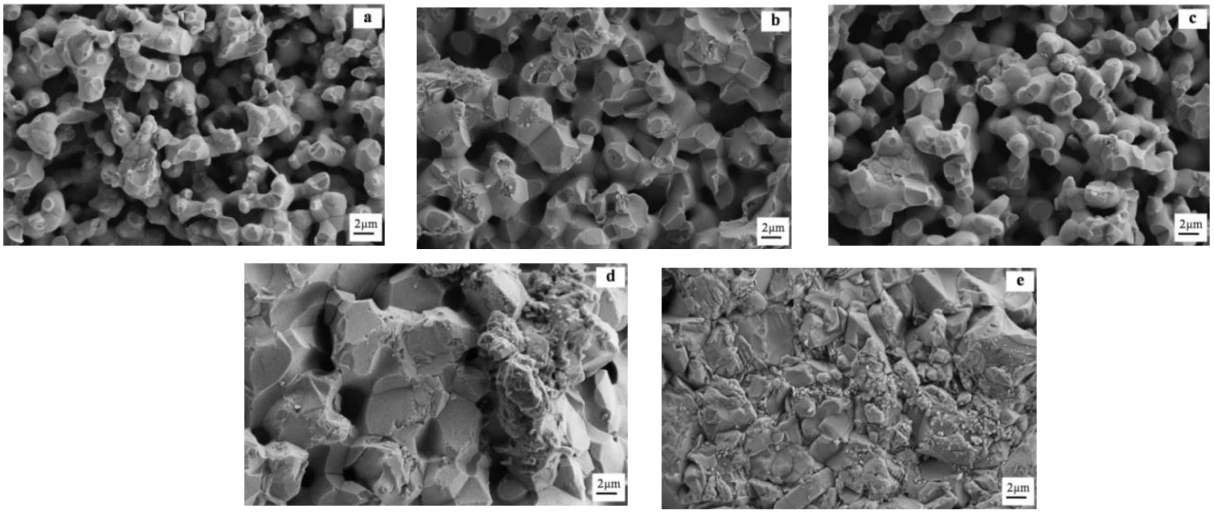

Figure 10. Surface morphology of sintered MgO-TCP after immersed in SBF for 3 weeks: (a) 1100°C; (b) 1150°C; (c) 1200°C, (d) 1250°C; and (e) 1300°C.

4. Conclusion

The effect of MgO dope β-TCP was investigated. The substituted of Mg^{2+} in β-TCP was confirmed by the peak shift in XRD result and the α- TCP phase was not presented in both TCP and MgO-TCP sintered sample for all sintering temperatures. The linear shrinkage and density and porosity showed better properties as increasing the temperature up to 1250°C meanwhile at the sintering temperature of 1300°C the MgO-TCP samples presented better properties. These suggest that due to the expansion of sintered TCP during high sintering temperature which causes micro-crack in the samples. The biological test revealed that both TCP and MgO-TCP can perform apatite layer on its surface for some sintering temperature which initially confirmed that these materials are biocompatible to use in the clinical application.

Acknowledgment

The authors gratefully acknowledge the financial support from ASEAN University Network/Southeast Asia Engineering Education Development Network (AUN/SEED-Net) of grant number 6050313.

References

[1] Famery M, Richard N and Boch P 1994 Ceramics International 20 327
[2] Ryu H S, Youn, H J, Hong K S, Chang B S, Lee C K and Chung S S 2002 Biomaterials 23 909
[3] Percival M 1999 Applied Nutritional Science Report 5 1
[4] Xue W, Dahlquist K, Banerjee A, Bandyopadhyay A and Bose S 2008 Journal of Materials Science: Materials in Medicine 19 2669
[5] Banerjee S S, Tarafder S, Davies N M, Bandyopadhyay A and Bose S 2010 Acta Biomaterialia 6 4167
[6] Standard test methods for apparent porosity, liquid absorption, apparent specific gravity, and bulk density of refractory shapes by vacuum pressure 2000 ASTM standard-C830
[7] Kokubo T and Takadama H 2006 Biomaterials 27 2907
[8] Implants for surgery-In vitro evaluation for apatite-forming ability of implant materials 2012 ISO 23317:2012(E)
[9] Kumar P N, Mishra S K and Kannan S 2015 Journal of Solid State Chemistry 231 13
[10] Kannan S, Neunhoeffer F G, Neubaure J, Pina S, Torres P M C, Ferreira J F 2010 Acta Biomaterialia 6 517
[11] Ahmad S I, Rao P K and Syed I A 2016 Journal of Taibah University for Science 10 381
[12] Syamimi N F, Matori K A, Lim W F, Aziz S A and Mohd-Zaid M H 2014 Journal of Spectroscopy 2014 1
[13] Ryu H S, Youn H J, Hong K S, Chang B S, Lee C K and Chung S S 2002 Biomaterials 23 909
[14] Qi G, Zhang S, Khor K A, Lye S W, Zeng X, Weng W, Liu C, Venkatraman S S and Ma L L 2008 Applied Surface Science 255 304
[15] Berg C 2017 UPTEC K 17021 Examensarbete 30 hp 3
[16] Kanchana P and Sekar C 2012 Journal of Minerals and Materials Characterization and Engineering 11 982
[17] Cheng P T 1989 Urolithiasis 225
[18] Bachra B N and Fischer H R A 1969 Calcified Tissue Research 3 248
[19] Xin R, Leng Y, Chen J and Zhang Q 2005 Biomaterials 26 6477
[20] Bachra B N and Fischer H R A 1969 Calcified Tissue Research 3 248